

## Near-threshold photoionization spectrum of aligned Ca $4s5p\ ^1P_1$

K. W. McLaughlin, D. S. Eschliman, O. P. Francis, and D. W. Duquette  
*Behlen Laboratory of Physics, University of Nebraska, Lincoln, Nebraska 68588-0111*  
 (Received 7 June 1993)

The relative cross section for photoionization from the  $4s5p\ ^1P_1$  excited level of neutral calcium has been measured using pulsed laser excitation and ionization of Ca atoms in an atomic beam. Photoelectrons are counted as a function of ionizing photon energy and polarization. Measurements cover the energy range from 51 300 to 51 700  $\text{cm}^{-1}$  above the Ca  $^1S_0$  ground state at a resolution of approximately 0.15  $\text{cm}^{-1}$ . The shapes and relative peak heights of resonances corresponding to the previously identified  $^3S_1$  and  $^3D_{1,2}$  autoionizing levels from the  $3d4d$  configuration have been determined. A new, extremely strong resonance is also evident at 51 467  $\text{cm}^{-1}$ , and it has been tentatively identified with the  $3d4d\ ^1P_1$  level. This is an experimental identification of a doubly excited even-parity singlet level in calcium.

PACS number(s): 32.80.Fb, 32.80.Dz

### INTRODUCTION

The experimental measurement of photoionization cross sections from excited states of neutral atoms has received increasing attention due to the use of tunable lasers as sources of excitation and ionization [1]. Excited atoms are rather easily prepared by polarized laser radiation in a wide variety of angular-momentum states and degrees of magnetic-substate alignment. This flexibility allows a correspondingly larger number of doubly excited (autoionizing) and continuum states to be studied than can be reached by one photon starting from the ground or metastable states. In addition, the cross sections for photoionization from an excited atomic state can be very large, around  $10^{-17}\ \text{cm}^2$ , and still larger within autoionizing resonances [2,3].

Techniques have been developed to measure both relative and absolute excited-state photoionization cross sections [4–6]. Photoionization from metastable excited states of the rare gases has been well studied using electron-impact excitation of the excited level with subsequent ionization by a tunable dye laser [7–9]. Absolute photoionization cross sections at a fixed ionization energy have been measured from short-lived excited states of He, K, Cs, and Rb excited from the ground state by resonance lines from a discharge lamp [10–13]. Other absolute measurements of total cross sections used tunable dye lasers to populate Cs  $7p\ ^2P$ , Rb  $6p\ ^2P$ , and Na  $4d\ ^2D$  and  $5s\ ^2S$  [14–16]. In these experiments, photoionization was performed at a fixed wavelength, even though some of the investigations utilized tunable lasers.

Measurements of the dependence of the cross section on ionizing photon energy are scarce. We have previously measured absolute cross sections for the Ti  $3d^24s4p\ ^3P_2$  level using laser excitation and ionization from 2990 to 6070  $\text{cm}^{-1}$  above threshold [3]. For Na  $3p\ ^2P$  excited by a cw dye laser, relative cross sections as a function of uv ionizing wavelength from a synchrotron have been measured [17]. The relative values were put on an absolute scale using a single measured cross section

near threshold. Combined laser-synchrotron measurements of this type have benefited from the introduction of undulators to increase the spectral fluence of the uv light from the synchrotron. The respective photon energies of lasers and synchrotrons complement each other as ionizing sources [18–20]. Other measurements of relative cross sections as a function of ionizing wavelength have been reported for Na and for Ca [21–23]. Using laser excitation from a measured density of ground-state atoms and laser ionization, the absolute photoionization cross sections of Ba  $6s6p\ ^1P_1$  and Mg  $3s3p\ ^1P_1$  were determined over a limited range of ionizing energy [24,25]. In the present investigation, relative excited-state photoionization cross sections from Ca  $4s5p\ ^1P_1$  are measured as a function of ionizing photon energy by observing the photoelectron yield normalized to the excited level fluorescence and ionizing laser intensity.

### EXPERIMENT

Figure 1 is a partial energy level diagram of Ca and  $\text{Ca}^+$  showing the important levels in this experiment. Calcium atoms in a thermal atomic beam are excited from the  $4s\ ^2S_0$  ground state to the  $4s5p\ ^1P_1$  level at 36 731  $\text{cm}^{-1}$  by a frequency-doubled pulsed dye laser. The excited atoms are photoionized by a second dye-laser pulse. Photoelectrons from  $\text{Ca}\ ^1P_1 + h\nu \rightarrow \text{Ca}^+\ ^2S_{1/2} + e^-$  are counted simultaneously with fluorescent photons at 672 nm from the spontaneous decay  $^1P_1 \rightarrow ^1D_2$ . The fraction of the excited-level population that is ionized is deliberately kept below 10%, so that the measured photoelectron signal is directly proportional to the photoionization cross section. Our technique is the same as that used to measure absolute cross sections in excited titanium [3] by depletion in fluorescence due to ionization. In the current Ca experiment, the ionizing photon wavelengths fall within the transmission band of the interference filter used to observe the 672-nm fluorescence line. Thus, in this ionizing energy region, we are unable to reliably observe fluorescence with the ionizing laser beam

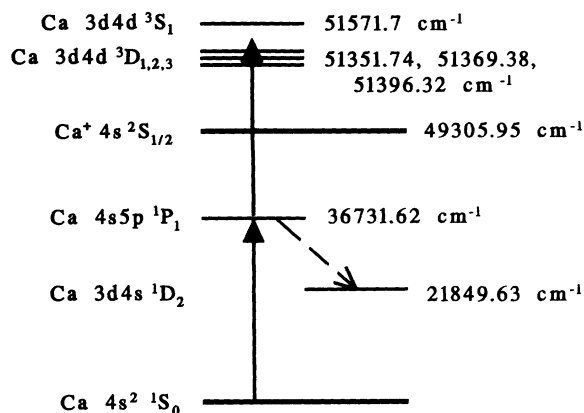


FIG. 1. Partial energy-level diagram for Ca and Ca<sup>+</sup> showing the energy levels important to this experiment. Transitions driven by lasers are indicated by a solid arrow. Spontaneous transitions are indicated by a dashed arrow. Configurations and terms are from Ref. [26].

present and so cannot put the relative cross sections on an absolute scale.

A schematic diagram of the experiment is shown in Fig. 2. Two independently tunable dye-laser oscillators and associated amplifiers are pumped by the same Continuum pulsed Nd:YAG (neodymium:yttrium aluminum garnet) laser at 10-Hz repetition rate. Both dye lasers are tuned by computer-controlled rotation stages. The excitation laser oscillator is a Pegasus DL102 producing an approximately 5-ns-long pulse with a spectral linewidth  $<0.1 \text{ cm}^{-1}$ . Pulses from the Pegasus oscillator are amplified twice and then frequency doubled in BBO ( $\beta$ -barium borate). The second dye laser oscillator is a custom, modified Littman design producing approximately 5-ns-long pulses with a somewhat larger ( $\approx 0.15 \text{ cm}^{-1}$ ) linewidth. These oscillator pulses are amplified one, two, or three times depending on ionizing flux requirements. The ionization laser pulse is optically delayed 15 ns so

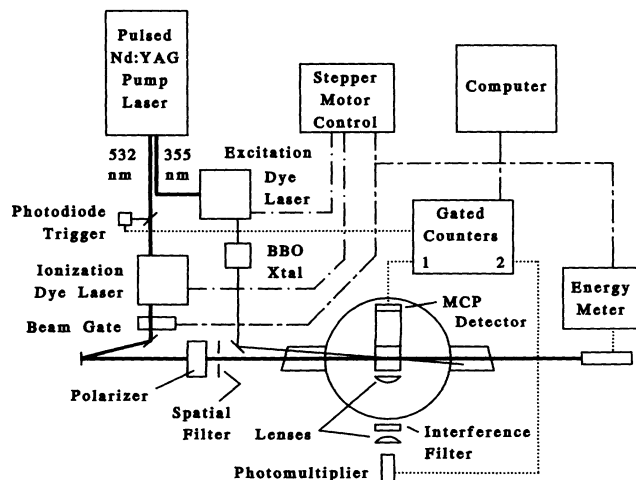


FIG. 2. Schematic diagram of experiment.

that the two beams do not overlap in time. At the entrance to the vacuum system the excitation beam is elliptical in shape with a major axis of approximately 1.5 mm. We spatially filter the ionization laser beam with a 0.5-mm pinhole and allow it to diverge over the optical delay path. The ionization-beam intensity profile at the entrance to the vacuum chamber consists of the central maximum of the Airy diffraction pattern of the spatial filter, with the diameter of the first dark ring approximately 1 cm. Both lasers are initially linearly polarized. We fix the polarization of the excitation laser to remain vertical and linear in all of these measurements. This is parallel to the atomic-beam axis and perpendicular to the fluorescence-photoelectron and laser-beam axes. The lower level for this transition is <sup>1</sup>S<sub>0</sub>, so that the excited <sup>1</sup>P<sub>1</sub> level is aligned into a purely  $m_J=0$  state ( $z$  axis vertical). The ionization laser polarizations used are (a) linear and parallel to excitation (vertical) and (b) right circularly polarized. Thus, the autoionizing and continuum states will also be aligned. In case (a), the resulting continuum states must have  $m_J=0$  ( $z$  axis vertical,  $z \perp k$ ). For case (b), it is more convenient to describe the <sup>1</sup>P<sub>1</sub> state in a coordinate system with the  $z$  axis along the propagation axis, which is common to both laser beams. With  $z = k$ , the vertical direction is now  $x$ , and the initial <sup>1</sup>P<sub>1</sub> level is a coherent superposition:  $(1/\sqrt{2})[|m_J = -1\rangle - |m_J = +1\rangle]$ . Then right circularly polarized ionization will produce states with  $m_J=0$  and  $+2$  ( $z$  axis horizontal,  $z \parallel k$ ). The difference between cases (a) and (b) yields information that is valuable in identifying the symmetries of autoionizing resonances.

The observed photoelectron counts are normalized to the excited-state fluorescence (with no ionization) and to the pulse energy per unit area of the center of the ionization beam. The two laser beams are directed nearly collinearly into the scattering region where they overlap on the Ca atomic beam. We are careful to align the laser beams so that the center of the broad, uniform ionization beam intersects the volume of excited Ca atoms. Immediately after the laser beams exit the scattering chamber, the ionization laser beam is directed to a Laser Precision pulse-energy meter with a precise 1-mm-diam circular entrance aperture. Random fluctuations in the number of excited atoms caused by drift in the Ca atom source or the excitation laser-pulse energy as well as in the ionization-laser energy are accounted for.

Figure 3 shows the Ca atomic-beam source and scattering region in more detail. The Ca atomic beam is produced from a simple cylindrical oven heated by a resistive element wound around the exterior. The oven is water-cooled from above so that the nozzle maintains the highest temperature. A thermocouple embedded in the heating element allows accurate determination of the element temperature. The atomic-beam nozzle is reentrant, so that the solid Ca metal is held below the nozzle entrance. We used this oven to produce a reliable Ca atomic beam for over 1000 h on a single 0.5-g charge of Ca. The uncollimated atomic beam is formed into an "outer" vacuum chamber. Interaction between the atoms and the laser beams takes place in an "inner" vacuum chamber that is separately pumped and isolated from the outer

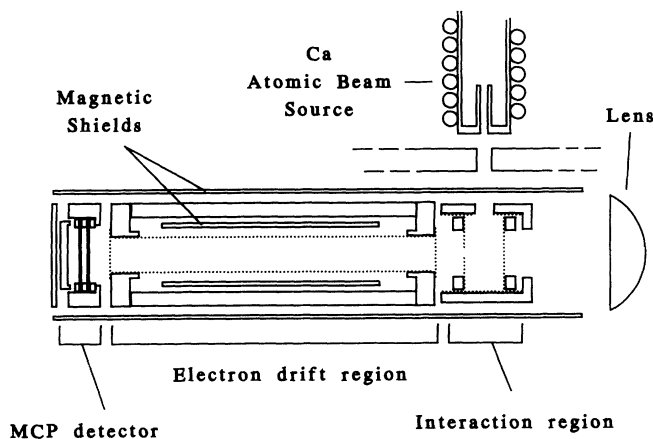


FIG. 3. Detail of Ca atomic-beam source, interaction region, and electron drift and detection regions. The laser-beam axis is normal to the page.

chamber except for a 2.0-mm-diam collimating aperture for the atomic beam. The base pressure in the inner chamber is  $5 \times 10^{-9}$  Torr and the pressure arises to  $< 10^{-7}$  Torr when the atomic-beam source is operating. The inner chamber contains the magnetically and electrically shielded interaction and electron collection regions and fluorescence collection optics.

Inside the inner chamber, the laser beams and atomic beam intersect at the center of a cylindrical interaction region formed by a 2.5-cm-diam Cu cylinder electrode and two Cu ring electrodes 1.2 cm apart. This intersection is at the focus of a two-lens,  $f/2.5$  fluorescence collection system with the optical axis orthogonal to the laser-beam and atomic-beam axes. Rejection of unwanted fluorescence and scattered laser light is provided by a narrow bandwidth interference filter placed between the pair of lenses. Photons from  $^1P_1 \rightarrow ^1D_2$  at 672 nm are detected by an EMR photon-counting photomultiplier. The signal is amplified and passed to one channel of a Stanford Research SR400 two-channel gated counter.

The ring electrodes support Mo mesh stretched across the open apertures, and the interior surface of the cylinder electrode is lined with Mo mesh. Opposite the fluorescence collection optics, the cylindrical region is coupled to a grounded, 10-cm time-of-flight drift region followed by a dual microchannel plate (MCP) electron detector. The drift region is also constructed of Mo mesh supported on a Cu frame. The ring electrode on this end of the interaction region supports a Mo disk with a 3.6-mm-diam aperture to define the angular acceptance of the drift region. For accumulation of total relative cross sections, we place potentials of  $-80$ ,  $-50$ , and  $-20$ -V on the photomultiplier tube end ring, cylinder, and MCP end ring, respectively, to pull all of the low-energy photoelectrons into the drift region. The  $-20$ -V difference between the MCP ring and the grounded entrance grid to the drift region serves to collimate the electrons and direct them toward the MCP detector. In this investigation there was no need to analyze the kinetic energy of the photoelectrons, since only the  $\text{Ca}^+ \ ^2S_{1/2}$  ground state is accessible. For "angle-differential" relative cross sec-

tions, we bias all electrodes at  $-50$  V so that the interaction region is essentially field free, while still maintaining the collimation and focusing at the entrance to the drift region. Electron counts are amplified and passed to the second channel of the SR400 gated counter.

Timing signals for the SR400 gates are provided by a fast photodiode observing a reflection from the pump laser. Data collection and experiment control are performed by an IBM PS/2. At approximately 30-s intervals the computer blocks or unblocks the ionization laser and periodically scans the excitation laser wavelength onto or off the  $\text{Ca} \ ^1S_0 \rightarrow \ ^1P_1$  transition. In this way, photoelectron counts and background counts are accumulated both with and without the production of excited Ca atoms. By taking differences of the counts acquired under different permutations of excitation and ionization, we accurately determined photoelectron counts that are solely due to ionization of the fluorescing excited level. Typical count rates are 1 to 5 fluorescent photons/s and 0.2 to 1 photoelectrons/s. Because the SR400 counter was gated to accept counts only for 100 ns after each laser pulse, the average background count rate was typically more than an order of magnitude below the average signal count rate.

## RESULTS

Figures 4–6 show the measured total and angle-differential cross sections for single-photon ionization of the  $4s5p \ ^1P_1$  excited level of Ca as a function of energy above the  $^1S_0$  Ca ground state for different ionizing laser polarization. The vertical scale is logarithmic due to the extreme variation in relative cross sections in this range. Uncertainty in the cross section obtained at each ionizing photon energy is indicated by the height of the box, representing plus or minus one standard deviation. The two major sources of this uncertainty are (i) accumulated statistical deviation in the photoelectron counts under the four permutations of excitation and ionization and (ii) a conservative estimate of  $\pm 20\%$  error in the measurement of the energy flux of the ionizing laser. The relative uncertainty in the ionizing photon energy is indicated by

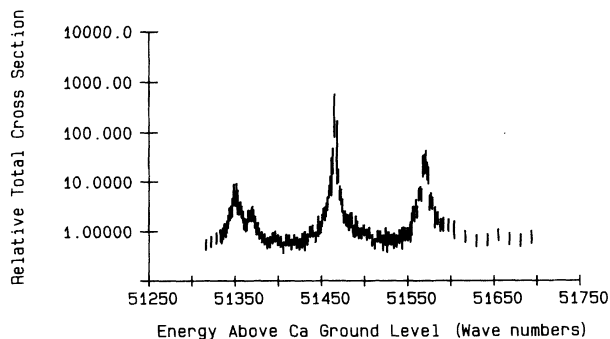


FIG. 4. Semilogarithmic plot of relative total photoionization cross section from  $\text{Ca} \ 4s5p \ ^1P_1$  using linearly polarized excitation and right circularly polarized ionization. The horizontal axis is energy in wave numbers above the  $\text{Ca} \ ^1S_0$  ground state.

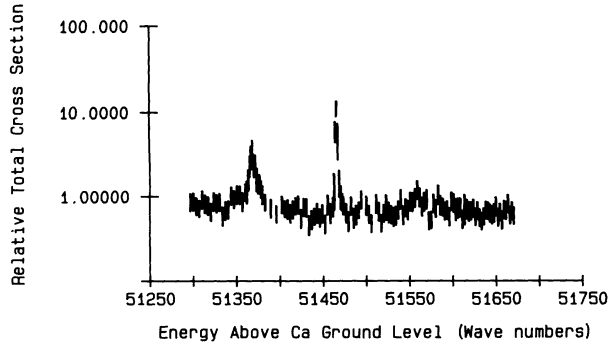


FIG. 5. Semilogarithmic plot of relative total photoionization cross section from Ca  $4s5p\ ^1P_1$  using linearly polarized excitation and parallel linearly polarized ionization. The horizontal axis is energy in wave numbers above the Ca  $^1S_0$  ground state.

the width of each box, typically twice the ionizing laser linewidth or  $\pm 0.3\text{ cm}^{-1}$ . On the scale of the figures this is too narrow to be seen clearly. Computer control of the laser wavelengths is repeatable to within a laser linewidth. The *absolute* uncertainty in the horizontal energy scale is less than  $\pm 5\text{ cm}^{-1}$  and is due entirely to the resolution limits of 0.25-m monochromator used. This uncertainty represents an overall displacement of the horizontal scale.

There are no other measurements with which to com-

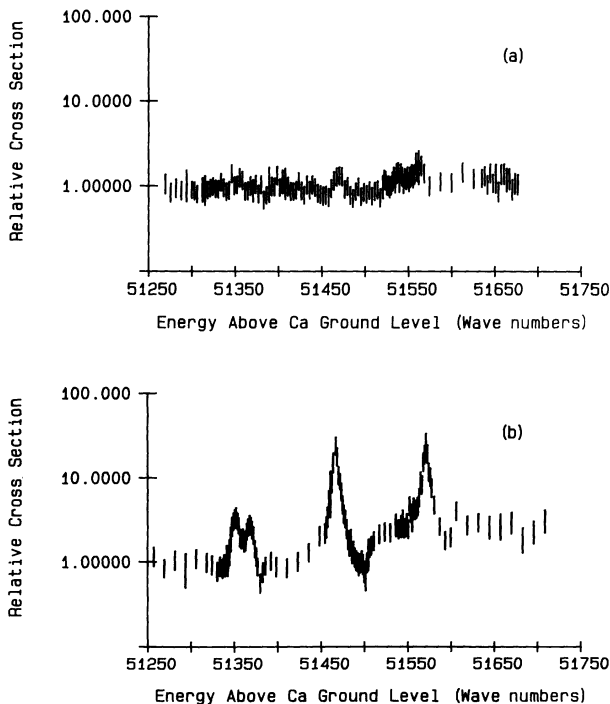


FIG. 6. Semilogarithmic plots of relative angle-differential cross section from Ca  $4s5p\ ^1P_1$  excited with linearly polarized light: (a) ionization linearly polarized and parallel, (b) ionization right circularly polarized. The horizontal axis is energy in wave numbers above the Ca  $^1S_0$  ground state.

pare the data in detail. Many triplet even-parity doubly excited states of calcium near the Ca<sup>+</sup>  $4s\ ^2S_{1/2}$  threshold have been previously identified [26]. In particular, the  $3d4d\ ^3D_{1,2}$  and  $^3S_1$  resonances appear prominently in our data at exactly the expected energies. The  $3dn\ ^1P$  series appears to be completely mixed into the  $4snp$  series [27] so transitions to  $3d4d$  are not surprising. Also, the  $4s5p\ ^3P_1$  level at  $36\,554.7\text{ cm}^{-1}$  may lend some triplet character to  $4s5p\ ^1P_1$ . None of the singlet levels of the  $3d4d$  configuration has been previously observed experimentally. Theoretical calculations of the positions of even singlet levels with  $J=0$  or  $2$  near the Ca<sup>+</sup> threshold exist but there are no calculations at present for the even singlet  $J=1$  levels [28].

Figures 4 and 5 show total relative cross sections obtained with different ionizing laser polarizations. In the data of Fig. 4 we have used right circular polarization to reach any  $0 \leq J \leq 2$  with  $m_J = 0, +2$ . Measurements at the center of the strong peak near  $51\,467\text{ cm}^{-1}$  have been omitted since the photoelectron detection system was saturated even at the lowest practicable excited Ca atom density and ionizing laser flux. In the data of Fig. 5 we have used linear ionizing polarization parallel to the excitation polarization to reach only  $m_J = 0$  and  $J = 0$  or  $2$ , since the Clebsch-Gordon coefficient  $\langle 1100|10 \rangle = 0$ . The difference in the two spectra is striking. The  $^3D_1$  and  $^3S_1$  resonances disappear in the parallel case, leaving  $^3D_2$  and a greatly reduced central peak. (The strong central peak appears with parallel polarization only because of a very small admixture of other polarizations in the ionizing laser beam). This clearly indicates that the strong peak near  $51\,467\text{ cm}^{-1}$  has  $J=1$ .

We have fit our data for total relative photoionization cross sections in Figs. 4 and 5 with the superposition of Fano-type autoionizing profiles plus a linearly varying background continuum. Since none of the resonances shows any clear asymmetry, we write the autoionizing profiles in the form

$$\sigma = \sigma_A q^2 \frac{\left(1 + \frac{E - E_c}{q\Gamma}\right)^2}{1 + \left(\frac{E - E_c}{\Gamma}\right)^2}. \quad (1)$$

For symmetric resonances, the absolute value of the parameter  $q$  is rather large. The peak relative cross section, given by  $\sigma_A q^2$ , is easily determined from our data, whereas  $q$  and  $\sigma_A$  separately are not. Fitted values of  $E_c$ ,  $\sigma_A q^2$ , and  $\Gamma$  for each resonance are shown in Table I.

In  $LS$  coupling the only Ca<sup>+</sup> ground-state continua accessible from  $4s5p$  are  $4ses\ ^1S_0$  or  $^3S_1$  and  $4sed\ ^1D_2$  or  $^3D_{1,2,3}$ . The widths of the three triplet resonances are fit best by values of  $\Gamma$  around  $3.5\text{ cm}^{-1}$ . These levels all have continua of the same  $LS$  symmetry into which to decay. On the other hand, the resonance at  $51\,466.7\text{ cm}^{-1}$  has a much smaller  $\Gamma$  of  $0.67\text{ cm}^{-1}$ . It seems likely therefore that the level here is  $^1P_1$ , for which there is no  $LS$  continuum of the same symmetry.

We have recorded angle-differential relative cross sections at a single angle for both of the laser polarizations

TABLE I. Values for  $E_c$ ,  $\sigma_A q^2$ , and  $\Gamma$  for each of four resonances obtained by fitting the data in Figs. 4 and 5 with Beutler-Fano profiles [Eq. (1)].

3d4d level	$E_c$ (cm <sup>-1</sup> )	$\Gamma$ (cm <sup>-1</sup> )	Circular polarization	Parallel polarization
			(Fig. 4) $\sigma_A q^2$ (relative)	(Fig. 5) $\sigma_A q^2$ (relative)
<sup>3</sup> D <sub>1</sub>	51 351.7	3.8	55	
<sup>3</sup> D <sub>2</sub>	51 369.4	3.6	20	30
<sup>1</sup> P <sub>1</sub> (tent.)	51 466.7	0.67	≈4000	150
<sup>3</sup> S <sub>1</sub>	51 571.6	3.1	250	

above in order to obtain an idea of the angular distribution of photoelectrons. Studies of angular distributions can be used to obtain very detailed information on the symmetry of the continuum and of autoionizing resonances [20,29,30]. Figure 6(a) shows the relative angle-differential cross section spectrum for parallel ionizing laser polarization. The spectrum is essentially featureless, including a lack of any peak associated with the <sup>3</sup>D<sub>2</sub> level. This would appear to indicate that the photoelectron angular distribution within this resonance is strongly peaked in the direction of the laser polarizations, at right angles to the collection angle. Figure 6(b) shows the angle-differential cross section spectrum for right circular ionizing laser polarization. Minima are clear on the high-energy side of all but the <sup>3</sup>D<sub>1</sub> resonance. The relative height of the <sup>1</sup>P<sub>1</sub> resonance is also much reduced. A definitive analysis of angular distributions will require further measurements.

## SUMMARY

We have measured the relative photoionization cross section of the aligned  $4s5p\ ^1P_1\ m_J=0$  excited level of Ca using two ionizing laser polarizations to selectively align the final states. The shapes of the three doubly excited autoionizing levels  $3d4d\ ^3D_{1,2}$  and  $3d4d\ ^3S_1$  have been determined from total relative cross-section spectra. An additional strong, narrow resonance at 51 466.7 cm<sup>-1</sup> has been observed and tentatively identified with the  $3d4d\ ^1P_1$  level.

## ACKNOWLEDGMENTS

This work is supported by the National Science Foundation, Grant No. PHY-9109164. We thank C. H. Greene and A. F. Starace for enlightening discussions.

- [1] R. N. Compton and J. C. Miller, in *Laser Applications in Physical Chemistry*, edited by D. K. Evans (Dekker, New York, 1989).
- [2] T. N. Chang, Phys. Rev. A **37**, 4090 (1988).
- [3] K. W. McLaughlin and D. W. Duquette, J. Opt. Soc. Am. B **9**, 1953 (1992).
- [4] K. D. Bonin, M. Gatzke, C. L. Collins, and M. A. Kadar-Kallen, Phys. Rev. A **39**, 5624 (1989).
- [5] S. L. Gilbert, M. C. Noecker, and C. E. Wieman, Phys. Rev. A **29**, 3150 (1984).
- [6] S. Kröll and W. K. Bischel, Phys. Rev. A **41**, 1340 (1990).
- [7] R. F. Stebbings, F. B. Dunning, F. K. Tittel, and R. D. Rundel, Phys. Rev. Lett. **30**, 815 (1973).
- [8] F. B. Dunning and R. F. Stebbings, Phys. Rev. A **9**, 2378 (1974).
- [9] R. D. Rundel, F. B. Dunning, H. C. Goldwire, Jr., and R. F. Stebbings, J. Opt. Soc. Am. **65**, 628 (1975).
- [10] V. P. Belik, S. V. Bobashev, and L. A. Shmaenok, Pis'ma Zh. Eksp. Teor. Fiz. **25**, 527 (1977) [JETP Lett. **25**, 494 (1977)].
- [11] K. J. Nygaard, R. J. Corbin, and J. D. Jones, Phys. Rev. A **17**, 1543 (1978).
- [12] A. N. Klyucharev and N. S. Ryazanov, Opt. Spektrosk. **32**, 1253 (1972) (USSR) [Opt. Spectrosc. **32**, 686 (1972)].
- [13] A. N. Klyucharev and V. Yu. Sepman, Opt. Spektrosk. **38**, 1230 (1975) (USSR) [Opt. Spectrosc. **38**, 712 (1975)].
- [14] U. Heinzmann, D. Schinkowski, and H. D. Zeman, Appl. Phys. **12**, 113 (1977).
- [15] R. V. Ambartsumian, N. P. Furzikov, V. S. Letokhov, and A. A. Puretsky, Appl. Phys. **9**, 335 (1976).
- [16] A. V. Smith, J. E. M. Goldsmith, D. E. Nitz, and S. J. Smith, Phys. Rev. A **22**, 577 (1980).
- [17] J. M. Preses, C. E. Burkhardt, R. L. Corey, D. L. Earsom, T. L. Daulton, W. P. Garver, J. J. Leventhal, A. Z. Msezane, and S. T. Manson, Phys. Rev. A **32**, 1264 (1985).
- [18] F. J. Wuilleumier, D. L. Ederer, and J. L. Picqué, Adv. At. Mol. Phys. **23**, 197 (1988).
- [19] M. Ferray, F. Gounand, P. D'Oliveira, P. F. Fournier, D. Cubaynes, J. M. Bizau, T. J. Morgan, and F. J. Wuilleumier, Phys. Rev. Lett. **59**, 2040 (1987).
- [20] M. Pähler, C. Lorenz, E. v. Raven, J. Rüder, B. Sonntag, S. Baier, B. R. Müller, M. Schulze, H. Staiger, P. Zimmermann, and N. M. Kabachnik, Phys. Rev. Lett. **68**, 2285 (1992).
- [21] H. T. Duong, J. Pinard, and J.-L. Vialle, J. Phys. B **11**, 797 (1978).
- [22] K. J. Nygaard, R. E. Hebner, Jr., J. D. Jones, and R. J. Corbin, Phys. Rev. A **12**, 1440 (1975).
- [23] K. Gerwert and K. J. Kollath, J. Phys. B **16**, L217 (1983).
- [24] A. Kallenbach, M. Kock, and G. Zierer, Phys. Rev. A **38**, 2356 (1988).
- [25] D. J. Bradley, C. H. Dugan, P. Ewart, and A. F. Purdie, Phys. Rev. A **13**, 1416 (1976).
- [26] J. Sugar and C. Corliss, J. Phys. Chem. Ref. Data, **14**, 51 (1985).
- [27] C. Froese Fischer and J. E. Hansen, J. Phys. B **18**, 4031

- (1985).
- [28] M. Aymar and M. Telmini, *J. Phys. B* **24**, 4935 (1991).
- [29] S. Baier, W. Fiedler, B. R. Müller, M. Schulze, P. Zimmermann, M. Meyer, M. Pahler, Th. Prescher, E. von Raven, M. Richter, J. Rüder, and B. Sonntag, *J. Phys. B* **25**, 923 (1992).
- [30] A. Siegel, J. Ganz, W. Bußert, and H. Hotop, *J. Phys. B* **16**, 2945 (1983).